

Online Adaptive Robust Tuning of PID Parameters

Ehsan Gholamzadeh Nabati* , Sebastian Engell*

** Process Dynamics and Operations Group
Department of Biochemical and Chemical Engineering
Technische Universität Dortmund
D-44221 Dortmund, Germany
e-mails: {ehsan.gholamzadeh-nabati; s.engell}@bci.tu-dortmund.de*

Abstract: In this paper, an online adaptation scheme for tuning of PID parameters is presented. This scheme is based upon our previous works on using a data-driven method to obtain a sufficient condition for robust stability and integrating robustness into the Unfalsified Control framework. Here, a modified bumpless transfer approach to facilitate the adaptation of the PID controller parameters is presented. The proposed scheme is demonstrated using a PID benchmark problem.

Keywords: Adaptive control, switching control, online controller optimization, PID control.

1. INTRODUCTION

A promising adaptive control approach is the Unfalsified Control, see Safonov and Tsao (1997). The key feature of this approach is the fact that very little knowledge about the plant is required a priori. Thus it can be easily applied to a large class of systems. Adaptation in Unfalsified Control is done by switching among a set of candidate controllers via the ϵ -hysteresis algorithm from Morse et al. (1992). In the original approach Wang et al. (2007), the so-called fictitious signals were used to evaluate the performance of the candidate controllers by means of a cost function.

However, as indicated by Dehghani et al. (2007) and Engell et al. (2007) the original cost function does not detect destabilizing controllers before they are placed in the control loop. An alternative cost function was proposed in Engell et al. (2007) which solved this problem.

To improve the set of candidate controllers, Engell et al. (2007) suggested to use this new cost function and the data recorded from measured signals in an online optimization to search for an optimal candidate controller. This idea has recently been extended to include a robustness constraint, which is only derived from the measurements data, to the optimization of the candidate controller parameters to obtain robust controllers. Also this condition is used to avoid non-robust controllers from been placed in the control loop, see Nabati and Engell (2010) and Nabati and Engell (2011).

This paper presents the application of our robust adaptive control scheme to online tuning of PID parameters. Here, an improved version of the bumpless transition approach of Cheong and Safonov (2008) to facilitate the adaptation of the PID controller parameters is presented.

The proposed scheme is demonstrated using the PID benchmark problem of Morilla (2011). Three simulations

are conducted. The first two simulations are the comparative tests suggested by Morilla (2011). Additionally, we propose a third simulation scenario to show the further potential of our adaptive control approach. The simulation results indicate considerable performance improvement in comparison with the non-adaptive reference case in all three scenarios.

The paper is organized as follows: First the proposed implementation of the PID controller and the main ideas of the adaptive Unfalsified Control framework with the extensions from Engell et al. (2007) are presented. In section 3, our proposed approach for inclusion of robustness in the Unfalsified Control framework is described. Section 4 shows the application of the scheme to the PID benchmark problem. The conclusions are drawn in section 5.

2. THE CONTROL SCHEME

2.1 Preliminaries

Let $\mathbf{x} := \{x(1), x(2), \dots \in \mathcal{R}\}$ denote discrete-time signals (sequences). The l_2 -norm of a sequence \mathbf{x} is defined as $\|\mathbf{x}\|_2 := (\sum_{k=0}^{\infty} |x(k)|^2)^{1/2}$ and the l_∞ -norm is defined as $\|\mathbf{x}\|_\infty := \max_{0 \leq k < \infty} |x(k)|$. Let \mathcal{G} be a dynamic operator which maps \mathbf{u} to \mathbf{y} , then $\mathbf{y} = \mathcal{G}(\mathbf{u})$ is written as $\mathbf{y} = \mathcal{G} \cdot \mathbf{u}$ if \mathcal{G} is linear. The induced 2-norm of a dynamic system \mathcal{G} is defined by $\|\mathcal{G}\|_{i2} := \sup_{\mathbf{u} \neq 0} \frac{\|\mathbf{y}\|_2}{\|\mathbf{u}\|_2}$. The signal-to-peak norm of a transfer function $T(s)$ is defined by $\|T(s)\|_l := \max_{0 \leq k < \infty} (\mathbf{w} T(k))$, where the row vector $T(k)$ is the step response of $T(s)$ and \mathbf{w} is a constant vector $\mathbf{w} := [-1, 1]^T$. π_k denotes the k step discrete time truncation operator $\pi_k : \{x(1), \dots\} \rightarrow \{x(1), \dots, x(k)\}$. \otimes denotes the convolution operator.

2.2 The controller structure and implementation

The transfer function of the PID controller is assumed to

be

$$C(s) = k_p \left(1 + \frac{1}{T_n s} + \frac{T_D s}{N s + 1} \right).$$

The parameters of the PID are adapted online. To facilitate the adaptation of the controller parameters, the PID controller is implemented in a specific setup. Fig. 1 presents the proposed implementation of PID controller. The specific placement of the PID gains shown in Fig. 1 helps to reduce the rapid changes in the control output u after switching the PID control parameters, see e.g Cheong and Safonov (2008). Furthermore, as shown in Fig. 1 the standard PID controller is complemented with an anti-windup mechanism to avoid the controller saturation.

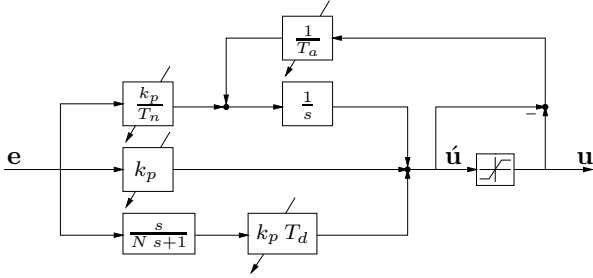


Fig. 1. Implementation of the PID controller with an anti-windup mechanism.

The parameters of the PID controller are adapted online by switching between a set of candidate controllers defined as $\mathbf{C} := \{C_1, C_2, \dots, C_n\}$. Each candidate controller C_i is a set of PID controller parameters defined as

$$C_i := [k_{p,i}, T_{n,i}, T_{d,i}]^T.$$

It is assumed that the time constant of the anti-windup term T_a is $T_a = T_{n,i}$ and the parameter N is fixed.

If switching of the PID controller parameters is not done properly, undesired bumps will occur immediately after the switching. A possible approach to avoid this problem is to change the internal states of the controller at the time of switching. The internal states of the PID controller can be changed, if the PID is implemented in the state space form as

$$\dot{x}_1 = \frac{k_p}{T_n} e, \quad (1)$$

$$\dot{x}_2 = -\frac{1}{N} x_2 + e, \quad (2)$$

$$u = x_1 - \frac{k_p T_d}{N^2} x_2 + \left(k_p + \frac{k_p T_d}{N} \right) e, \quad (3)$$

where x_1 and x_2 are the states of the integrator and derivator of the PID controller respectively.

To achieve a bumpless transfer, the states x_1^+ and x_2^+ can be manipulated at the time of switching to the *new* parameters (k_p^+, T_n^+, T_d^+) such that the control output remains constant after the swithing

$$u^+ = u. \quad (4)$$

Here, we present an improved version of the approach in Cheong and Safonov (2008) to manipulate the internal states of the controller. This approach is based on the slow fast decomposition method of Balas et al. (2005). According to the slow-fast decomposition method, the PID controller can be decomposed into a slow “integrator” part and a fast “derivator” part.

Cheong and Safonov (2008) suggested to set the state of the fast part to zero $x_2^+ = 0$ and recalculate the state of the slow part of the controller to achive $u^+ = u$. An equation for x_1^+ is obtained from (3) and (4) as

$$x_1^+ + \left(k_p^+ + \frac{k_p^+ T_d^+}{N} \right) e = x_1 - \frac{k_p T_d}{N^2} x_2 + \left(k_p + \frac{k_p T_d}{N} \right) e,$$

where $x_2^+ = 0$ and solving for x_1^+ results in

$$x_1^+ = x_1 + \left(k_p - k_p^+ + \frac{k_p T_d}{N} - \frac{k_p^+ T_d^+}{N} \right) e - \left(\frac{k_p T_d}{N^2} \right) x_2. \quad (5)$$

Based on several experiments, we noticed that a better practice to achieve a bumpless transfer is to maintain the state of the fast part of the controller $x_2^+ = x_2$ and recalculate the state of the slow part in a different fashion than suggested by Cheong and Safonov (2008). In our proposed bumpless transition approach the new states of the PID controller after the switching are calculated from

$$x_1^+ = x_1 + \left(k_p - k_p^+ + \frac{k_p T_d}{N} - \frac{k_p^+ T_d^+}{N} \right) e - \left(\frac{k_p T_d}{N^2} - \frac{k_p^+ T_d^+}{N^2} \right) x_2, \quad (6)$$

$$x_2^+ = x_2, \quad (7)$$

Equation (6) is derived from (4) assuming that at the time of switching $x_2^+ = x_2$. The equations (6) and (7) are different from those in Cheong and Safonov (2008) where the term $\frac{k_p^+ T_d^+}{N^2}$ in (6) is not considered and x_2^+ is equal to zero.

2.3 The adaptive control scheme

Fig. 2 shows the setup of our adaptive control scheme. This setup is a modification of the scheme in Wonghong and Engell (2008). The unknown plant \mathbf{P} is controlled in a feedback loop. The online supervisor modifies the parameters of the active controller \hat{C} by selecting the best candidate controller from the set of candidate controllers \mathbf{C} . If a suitable candidate controller is not available, an online optimization is performed and new candidate controllers are added to the set \mathbf{C} .

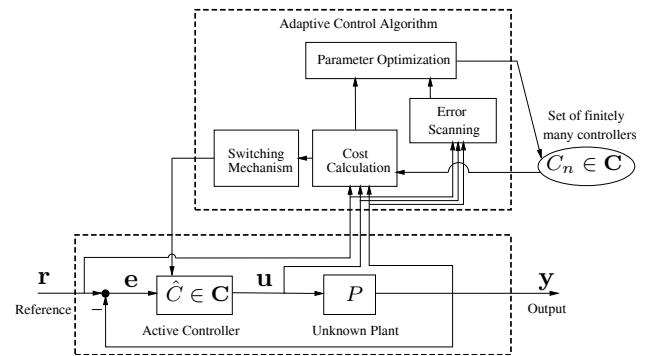


Fig. 2. The adaptive control scheme

The adaptation of the active controller is based on the ϵ -hysteresis algorithm of Morse et al. (1992). This algorithm is widely used in the Unfalsified Control framework, see e.g. Wang et al. (2007). In ϵ -hysteresis algorithm, at each time step k , the obtained measurements $(\mathbf{r}, \mathbf{u}, \mathbf{y})$ are used in a cost function $J(C_i, k)$ to compute the cost of each candidate controller. If a candidate controller C_i exists that *can* perform better than the active controller \hat{C} ,

$$J(\hat{C}, k) > \min_{C_i \in \mathbf{C}} J(C_i, k) + \epsilon, \quad (8)$$

then C_i is selected as the active controller and is placed in the control loop in the next time step, $\hat{C} := \arg \min_{C_i \in \mathcal{C}} J(C_i, k)$.

The threshold ϵ is used to ensure that the adaptation is not performed continuously but only when necessary. By selecting a proper threshold α and monitoring the candidate controllers at each time step, destabilizing candidate controllers can be detected. Thus, if

$$J(C_i, k) > \alpha, \quad (9)$$

the candidate controller C_i is called falsified and removed from the set of candidates, see Safonov and Tsao (1997).

Following the Unfalsified Control idea, the so-called fictitious signals are used to evaluate a measure for the performance of the candidate controllers. Fig. 3 shows the setup to calculate the fictitious reference $\tilde{\mathbf{r}}_i$ and the fictitious error $\tilde{\mathbf{e}}_i$ signals for each candidate controller C_i . Here C_i^{-1} denotes the inverse transfer function of the controller C_i .

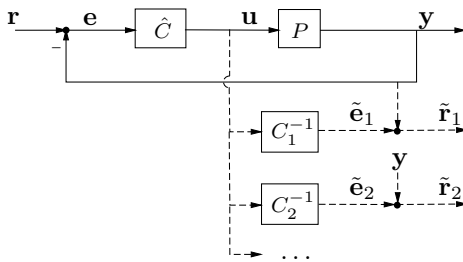


Fig. 3. Generation of fictitious signals $\tilde{\mathbf{r}}_i, \tilde{\mathbf{e}}_i$.

Originally, the signals $\tilde{\mathbf{r}}_i, \tilde{\mathbf{e}}_i$ were used directly in a cost function to compute the cost values, see Safonov and Tsao (1997), Wang et al. (2007). However, as indicated in Dehghani et al. (2007), Engell et al. (2007) the originally proposed cost function can not compute the cost of the destabilizing controllers correctly unless the destabilizing controller is placed in the control loop. Therefore, in Engell et al. (2007) a new cost function that can be used to evaluate the performance of both stabilizing and destabilizing candidate controllers correctly was suggested. This new cost function which is also used here is defined by

$$J(C_i, k) := \frac{\|\pi_k \mathbf{e}_i\|_2}{\|\pi_k \mathbf{r}\|_2 + \rho}, \quad (10)$$

where \mathbf{e}_i is the control error that would result if the candidate controller C_i was in the loop instead of the active controller \hat{C} until time k .

For a linear system, the control error \mathbf{e}_i and reference signal \mathbf{r} are related by the sensitivity transfer function $S_i := \frac{1}{1+P C_i}$ as $E_i(z) := S_i(z) R(z)$ or similarly as $\tilde{E}_i(z) := S_i(z) \tilde{R}_i(z)$. As the plant P is unknown, S_i and therefore the control error \mathbf{e}_i can not be computed directly. To solve this issue, in Engell et al. (2007) it was suggested to compute the impulse response of S_i approximately by deconvolution of the fictitious signals $\tilde{\mathbf{r}}_i$ and $\tilde{\mathbf{e}}_i$, using $\mathbf{e}_i := \tilde{\mathbf{s}}_i \otimes \mathbf{r}$ and $\tilde{\mathbf{e}}_i := \tilde{\mathbf{s}}_i \otimes \tilde{\mathbf{r}}_i$.

In Engell et al. (2007) and Wonghong and Engell (2008) it was suggested to use the cost function (10) in an online optimization to compute l_2 -optimal controllers. This idea is followed here.

As shown in Fig. 2, two separate online mechanisms can trigger the optimization in our scheme. The cost mon-

itoring mechanism calculates the cost of all candidate controllers. It triggers the optimization if all candidate controllers are falsified. The error scanning mechanism monitors the error \mathbf{e} and rate of change of error to determine whether the active controller (which is the best available controller in the set) is performing satisfactorily or not. If the active controller is not performing satisfactorily (e.g. in case of non-decreasing steady state error), the error scanning mechanism triggers the optimization, see Nabati and Engell (2010) for details.

3. INCLUSION OF ROBUSTNESS

If the unknown plant is nonlinear and/or time-varying, the information gained from the signals $(\mathbf{r}, \mathbf{u}, \mathbf{y})$ recorded in the past at some operating point does not represent the behavior of the plant fully and correctly. Thus there is a mismatch between the plant dynamics that is extracted from the recorded signals and the true plant dynamics. Hence robustness against uncertainties must be included.

To include robustness against uncertainties into adaptive control scheme, we propose to use a data-driven method to derive bounds for the uncertainties. Based on the obtained bounds, a sufficient condition for robust stability is defined. This condition is used as a constraint in the optimization to obtain optimal controllers which are robust for the observed plant-model mismatch and in the controller falsification to avoid non-robust controllers from being placed in the control loop, see Nabati and Engell (2010), and Nabati and Engell (2011).

To describe the uncertainties, the model error modeling concept of Ljung (1999) which is shown in Fig. 4 is employed.

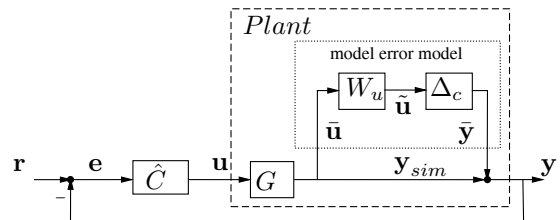


Fig. 4. Output-multiplicative uncertainty description.

In this concept, a general nonlinear plant P is described by a linear model G and a nonlinear model error model. Since the plant P is unknown, the linear model G has to be obtained from the recorded signals $(\mathbf{r}, \mathbf{u}, \mathbf{y})$ using a closed-loop identification technique. We propose that during each call of the optimization algorithm a *new* linear model G for the plant is identified.

The model error model part consists of an arbitrarily selected linear filter W_u and the operator Δ_c which maps $\tilde{\mathbf{u}}$ to $\tilde{\mathbf{y}}$. The signal $\tilde{\mathbf{u}} = \mathbf{y}_{sim}$ is obtained by simulation as $\mathbf{y}_{sim} = G \cdot \mathbf{u}$ and similarly $\tilde{\mathbf{u}} = W_u \cdot \tilde{\mathbf{u}}$.

Based on the small gain theorem, the system shown in Fig. 4 remains stable for all possible uncertainties described by the output-multiplicative uncertainty setup, if the condition

$$\|T_{\tilde{\mathbf{u}}\tilde{\mathbf{y}}}\|_\infty \cdot \|\Delta_c\|_\infty < 1, \quad (11)$$

holds. Where $T_{\tilde{\mathbf{u}}\tilde{\mathbf{y}}}$ is the transfer function between $\tilde{\mathbf{y}}$ and $\tilde{\mathbf{u}}$.

To evaluate (11) it is necessary to select a filter W_u and determine the gain of Δ_c . To select the filter W_u we follow Hindi et al. (2002) and Völker and Engell (2005). Where the idea is to use an optimization to compute W_u such that a tight uncertainty model is obtained which is consistent with the measurements. Afterwards, the gain of Δ_c is obtained following Poolla et al. (1994).

Theorem 1. Poolla et al. (1994). Given input and output sequences $\tilde{\mathbf{u}}, \tilde{\mathbf{y}}$ of length N , there exists a stable causal dynamic system Δ_c with

$$\|\Delta_c\|_{i2} \leq \gamma, \quad (12)$$

iff

$$\|\pi_k \tilde{\mathbf{y}}\|_2 \leq \gamma \|\pi_k \tilde{\mathbf{u}}\|_2, \quad \forall k \in [1, N]. \quad (13)$$

Theorem 1 gives an upper bound γ , for the gain of the operator Δ_c . The minimum value of γ clearly is

$$\gamma_{min} = \max_{k=1..N} \frac{\|\pi_k \tilde{\mathbf{y}}\|_2}{\|\pi_k \tilde{\mathbf{u}}\|_2}. \quad (14)$$

We propose that during each call of the optimization algorithm, the approach of Völker and Engell (2005) is employed and a *new* filter W_u that provides a tight uncertainty bound in combination with the *new* linear model G is obtained.

Using γ_{min} , the obtained filter W_u is scaled in each time step according to algorithm 1 such that $\|\Delta_c\|_\infty \leq 1$ holds. Thus a sufficient condition for robust stability is obtained as

$$\left\| \frac{-W_u G C_i}{1 + G C_i} \right\|_\infty < 1. \quad (15)$$

This inequality has to be evaluated in the frequency domain. It is used as a constraint in the optimization and in the controller falsification.

3.1 Multi objective optimization

In order to obtain robust controllers, we propose a multi objective optimization to replace the l_2 based optimization scheme of Engell et al. (2007). This multi objective optimization is done online, when it is triggered as described in section 2.3. When the optimization is activated, all data collected from the measurements are divided into two parts. From the first part, a nominal model of the plant G is identified. The nominal model along with the second part of the measurements are used to obtain the linear filter W_u . The model G and the filter W_u are used to solve the optimization problem, see Nabati and Engell (2010) and Nabati and Engell (2011) for details. The new optimization is formulated as

$$\min_{\theta} \left\| \frac{1}{1 + G C_\theta} \right\|_2, \quad (16)$$

$$s.t. \left\| \frac{C_\theta}{1 + G C_\theta} \right\|_l < \gamma_l, \quad (17)$$

$$s.t. \left\| \frac{-W_u G C_\theta}{1 + G C_\theta} \right\|_\infty < \gamma_\infty, \quad (18)$$

$$\text{and } \theta \in \mathbf{P}_1 \times \mathbf{P}_2 \times \dots, \quad (19)$$

where θ represents the parameters of the controller C , $\gamma_l := [-u_{min}, u_{max}]^T$ is the bound for the control output and $\gamma_\infty \leq 1$ parametrizes the robustness constraint.

After each optimization, the resulting optimal controller is set as the active controller and is added to the set of candidate controllers.

Algorithm 1 Δ_c consistency test

- 1: **initialize:** Let $k := k_0$ be the time when Alg. 1 is called for the first time; let $\mathbf{y} := \{y(0), \dots, y(k)\}$, $\mathbf{u} := \{u(0), \dots, u(k)\}$ be measurements
 - 2: $k := k + 1$
 - 3: $\tilde{\mathbf{y}} := \mathbf{y} - G \cdot \mathbf{u}$
 - 4: $\tilde{\mathbf{u}} := W_u \cdot G \cdot \mathbf{u}$
 - 5: $\gamma := \max(\|\pi_k \tilde{\mathbf{y}}\|_2 / \|\pi_k \tilde{\mathbf{u}}\|_2, 1)$
 - 6: $W_u := \gamma \cdot W_u$
 - 7: **goto 2**
-

3.2 New conditions for controller falsification

In the original Unfalsified Control approach falsification of the candidate controllers is only based on the condition (9). Non-robust controllers are not prevented from being placed in the control loop. To overcome this problem, we proposed in Nabati and Engell (2010) to augment the candidate controller falsification condition by an \mathcal{H}_∞ robustness criterion as

$$J(C_i, k) > \alpha, \quad (20)$$

or

$$\left\| \frac{-W_u G C_i}{1 + G C_i} \right\|_\infty > 1. \quad (21)$$

Both conditions (20) and (21) are evaluated at each time step for each C_i . If for a C_i , one of these conditions holds that controller is falsified.

The cost function $J(C_i, k)$ in condition (20) is evaluated using an FIR model of \tilde{S}_i which is computed at each time step by deconvolution, see Engell et al. (2007). Thus the computed cost value reflects the performance of the candidate controller at the current operating conditions accurately. Having an accurate cost value improves the adaptation using the ϵ -hysteresis algorithm.

To reduce the computational effort, the condition (21) is calculated using a fixed linear plant model G and a fixed filter W_u which were obtained during the last call of the optimization algorithm. G and W_u are updated again if an optimization is activated. Thus, the only term in (21) which is updated at each time step is the gain of the filter W_u . It is updated according to algorithm 1.

4. APPLICATION TO A BENCHMARK PROBLEM

The benchmark problem of Morilla (2011) is presented here as an example. In this benchmark problem, an industrial drum boiler is controlled with a PID controller. The schematic of the drum boiler is shown in Fig. 5.

For a proper operation of the drum boiler, it is necessary to control the fuel/air ratio, the level of water in the drum and the steam pressure. According to Morilla (2011), the fuel/air ratio is regulated by a air control subsystem and the level of water in the drum is regulated by the feedwater control subsystem. Thus, the drum boiler can be presented

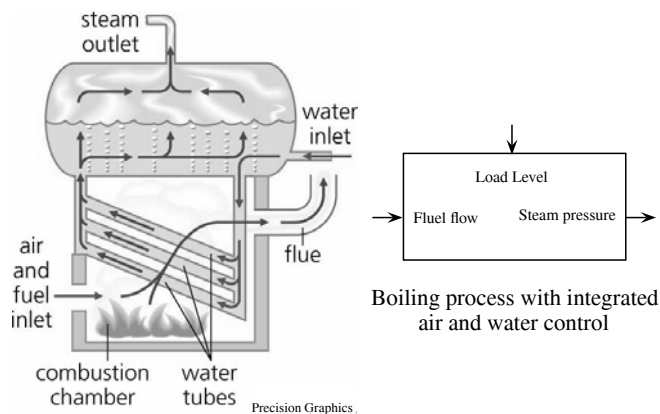


Fig. 5. Schematic of a drum boiler (left) and the process presentation as a SISO system (right).

as a SISO system shown in Fig. 5. In this SISO system, the steam pressure $\mathbf{y} := \text{Steam Pressure}$ is controlled by the fuel flow $\mathbf{u} := \text{Fuel Flow}$. The load level act as a disturbance on the system.

A black box model of the boiler is provided by Morilla (2011) as a Matlab[®] Simulink file. We use a PID controller with an anti windup mechanism shown in Fig. 1 to control the model of the boiler. The parameters of the PID controller are adapted online via our adaptive control scheme shown in Fig. 2 using the measured signals $(\mathbf{r}, \mathbf{u}, \mathbf{y})$. The proposed bumpless transfer approach is employed to achieve a smooth transition between the controllers.

Three simulations are conducted. The first two simulations are the comparative tests suggested by Morilla (2011). Additionally, we propose a third simulation scenario to show the further potential of our adaptive control approach.

The initial operating point of the boiler in all simulations is given as: Fuel flow = 35.21%, Load level = 46.36%, Steam pressure = 60%.

The control sampling period is 5 sec in all simulations. The model is integrated continuously. A zero order hold is used between the controller and the model. The control input has to be in the range $0\% \leq \mathbf{u} \leq 100\%$. It is assumed that the control parameters T_D, N are $T_D = 0$ and $N = 0.01$. The remaining control parameters $\theta := [k_p, T_n]^T$ are adapted online using our adaptive control scheme. The simulations are done on an Intel[®]E2180 with 2GB RAM.

The candidate controllers set consists of four controllers

$$\mathbf{C} := \{[2.5, 50]^T, [2.5, 25]^T, [5, 50]^T, [5, 25]^T\}. \quad (22)$$

The controllers in the set \mathbf{C} are combinations of the reference and the example PID controllers given in Morilla (2011). In all simulations, initially the plant is under operation with the reference controller $[2.5, 50]^T$.

4.1 Comparative test 1

In this test, a time variable disturbance (load level) shown in Fig. 8 acts on the system. This disturbance causes the steam pressure to deviate from its setpoint at 60% as shown in Fig. 6. This figure shows that the reference controller does not perform well.

As shown in Fig. 7, after 410 sec our adaptive control scheme detect that a candidate controller $[5, 25]^T$ which can perform better than the reference controller exists and switches to it. Fig. 6 clearly shows the achieved improvement of the controller performance after 410 sec. It can be seen that transition between the two controllers is bumpless. This simulation took 33 seconds.

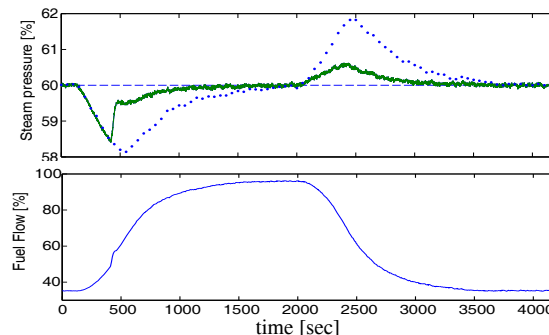


Fig. 6. Comparative test 1: System reference (top, dashed), system output for the adaptive case (top, line), system output for the reference case (top, dotted), the manipulated variable (bottom).

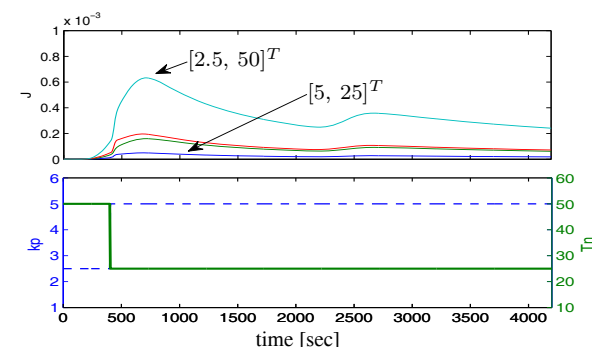


Fig. 7. Comparative test 1: Cost of the candidate controllers (top), adaptation of the controller gain k_p (bottom, dashed) and time constant T_n (bottom, line).

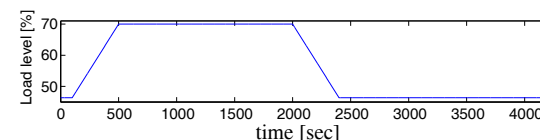


Fig. 8. Comparative test 1: Load level.

4.2 Comparative test 2

In this test, the load level is fixed at 46.36%. As shown in Fig. 9, the set point of the steam pressure changes from 60% to 65%. This figure shows that the reference controller does not perform well in this scenario too.

As shown in Fig. 10, after 120 sec our adaptive control scheme switches to $[5, 50]^T$ and after 145 sec to $[5, 25]^T$. This adaptation improves the controller performance comparing to the reference case as shown in Fig. 9. This simulation took 15 seconds.

4.3 Test 3

The goal of this simulation is to show that our adaptive control scheme can tune the active controller even in the

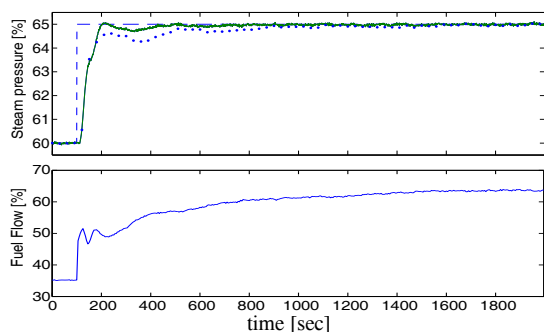


Fig. 9. Comparative test 2: System reference (top, dashed), system output for the adaptive case (top, line), system output for the reference case (top, dotted), the manipulated variable (bottom).

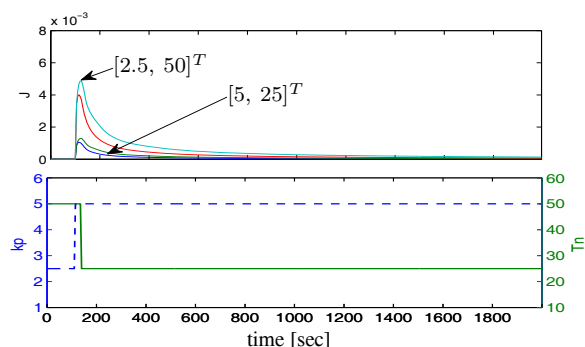


Fig. 10. Comparative test 2: Cost of the candidate controllers (top), adaptation of the controller gain k_p and time constant T_n (bottom).

case that initially no good candidate controller is available. Here, the initial candidate controllers set consists only of the reference controller $[2.5, 50]^T$. In this test, a time variable set point trajectory for the steam pressure is considered, see Fig. 11.

The error scanning mechanism activates the optimization four times. The collected measurements are used in the optimization to add new candidate controllers to the set. The obtained optimal controllers are used to tune the active controller parameters as shown in Fig. 11. This figure shows that the system performance is improved by adaptation of the PID parameters. This simulation took 1003 seconds in total. Each of four optimizations took about 120 seconds.

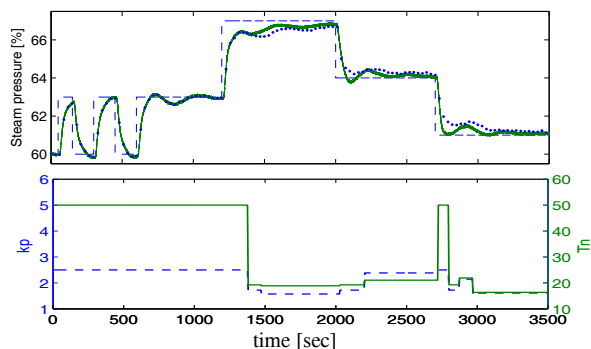


Fig. 11. Test 3: System reference (top, dashed), system output for the adaptive case (top, line), system output for the reference case (top, dotted), adaptation of the controller gain k_p (bottom, dashed) and time constant T_n (bottom, line).

5. CONCLUSION

In the presented work, an online adaptation scheme for PID parameters is developed. An improved bumpless transition approach to facilitate the adaptation of the PID controller parameters is presented. The proposed adaptive scheme is applied to a PID benchmark problem. The results indicate considerable performance improvement in comparison with non-adaptive reference case in all three simulations. The achieved improvement was obtained without making any assumption about the plant nor conducting any identification tests prior to the simulations. The computation times indicate that the presented approach can be applied to the real process.

REFERENCES

- Balas, G.J., Chiang, R.Y., Packard, A.K., and Safonov, M.G. (2005). Robust control toolbox. *MathWorks*, 641 pages.
- Cheong, S.Y. and Safonov, M.G. (2008). Bumpless transfer for adaptive switching controls. *IFAC World Congress*, 14415–14420.
- Dehghani, A., Anderson, B.D.O., and Lanzon, A. (2007). Unfalsified Adaptive Control: A New Controller Implementation and Some Remarks. *Euro. Cont. Conf.*, 709–716.
- Engell, S., Tometzki, T., and Wonghong, T. (2007). A New Approach to Adaptive Unfalsified Control. *European Control Conf.*, 1328–1333.
- Hindi, H., Seong, C.Y., and Boyd, S. (2002). Computing optimal uncertainty models from frequency domain data. *IEEE Conf. on Decision and Control*, 2898–2905.
- Ljung, L. (1999). Model validation and model error modeling. *Proc. Åström symposium on control*, 15–42.
- Morilla, F. (2011). Benchmark for pid control based on the boiler control problem. <http://www.dia.uned.es/~fmorilla/benchmarkPID2012/>.
- Morse, A.S., Mayne, D.Q., and Goodwin, G.C. (1992). Application of hysteresis switching in parameter adaptive control. *IEEE Trans. Automatic Control*, 37, 1343–1354.
- Nabati, E.G. and Engell, S. (2010). An Improved Adaptive Control Algorithm Based Upon Unfalsified Control. *IFAC ALCOSP Workshop*, 174–179.
- Nabati, E.G. and Engell, S. (2011). Data-Driven Adaptive Control: Making Unfalsified Control Work Better. *Proc. IFAC World Congress*, 1285–1290.
- Poolla, K., Khargonekar, P., Tikku, A., Krause, J., and Nagpal, K. (1994). A time domain approach to model validation. *IEEE Trans. Automatic Control*, 39, 951–959.
- Safonov, M.G. and Tsao, T.C. (1997). The unfalsified control concept and learning. *IEEE Trans. Autom. Control*, 42, 843–847.
- Völker, M. and Engell, S. (2005). Computation of Tight Uncertainty Bounds from Time domain Data with Application to a Reactive Distillation Column. *IEEE Conf. on Decision and Control*, 2939–2944.
- Wang, R., Paul, A., Stefanovic, M., and Safonov, M.G. (2007). Cost-detectability and Stability of Adaptive Control Systems. *Int. J. Robu. Nonlin. Cont.*, 549–561.
- Wonghong, T. and Engell, S. (2008). Application of a New Scheme for Adaptive Unfalsified Control to a CSTR. *Proc. IFAC World Congress*, 13247–13252.